QUANTIFY
QUantum EnhANced PhoTonic Integrated Sensors For MetrologY

Report on TPOC stability assessment using squeezed state of light

D4.2

Grant Agreement No.	101135931
Project Start Date	01.01.2024
Duration of the project	42 months
Deliverable Number	D4.2
Deliverable Leader	CSEM SA
Dissemination Level (PU, SEN)	PU
Status	Final version
Submission Date	04.05.2026
Author **Institution** **Email**	Thibault Voumard CSEM SA thibault.voumard@csem.ch

Funded by the European Union

This project has received funding from the European Union's Horizon Europe research and innovation programme under grant agreement N° 101135931.
The opinions expressed in this document reflect only the author's view and in no way reflect the European Commission's opinions. The European Commission is not responsible for any use that may be made of the information it contains.

Modification Control

VERSION	DATE	DESCRIPTION AND COMMENTS	AUTHOR
0.1	22.12.2025	First Draft	Thibault Voumard CSEM SA
0.2	15.01.2026	Version for CSEM internal review	Thibault Voumard CSEM SA
0.3	20.02.2026	CSEM's internally reviewed version, ready for project partner review	Thibault Voumard CSEM SA
0.4	06.03.2026	Version amended following review by project partner.	Thibault Voumard CSEM SA
1.0	04.05.2026	Version amended following review by project coordinator.	Thibault Voumard CSEM SA

List of contributors

- Thibault Voumard
- Laurent Balet
- Sylvain Karlen
- Davide Grassani
- Axel Schönbeck – Internal reviewer
- Salvatore Micalizio – Internal reviewer
- Giulia Aprile – Internal reviewer

List of Acronyms

Acronym	Full name
CA	Consortium Agreement
CFS	Certificate on the Finance Statement
CSOC	Chip-Scale Optical Clock
MEMS	Micro-ElectroMechanical Systems
PICSq	Photonic Integrated Circuit Squeezer
SHG	Second Harmonic Generation
SPDC	Spontaneous Parametric Down-Conversion
SWaP	Size Weight and Power

Table of Contents

1. Introduction

1.1 Purpose of this document

The QUANTIFY project aims to advance sensing technologies through the development of MEMS atomic vapor cell technology (MEMS cells) and photonic integrated light sources, including the development of a quantum-enhanced optical atomic clock using a photonic squeezer (PICSq). The purpose of this document is to assess the theoretical stability enhancement provided to a two-photon Rubidium clock by using squeezed states of light. First, the quantum enhancement to the fluorescence photon rate is computed, to assess potential improvements in compactness, power consumption and long-term stability of the clock. Secondly, the effects of squeezed light on intermodulation noise are investigated, with potential improvements on the short-term stability.

1.2 State of art and status of exploited technology

Enhancement of spectroscopic signals using squeezed light has been reported in specific experimental conditions with low photon counts [1-7]. However, in situations akin to a high atomic count (such as a Rubidium vapor cell) illuminated with a high photon count, no significant quantum enhancement has yet been observed [8-13] or can be fully attributed to quantum light. To assess the potential improvements to the stability of two-photon Rubidium clocks, the full electromagnetic quantum scattering cross-section is computed for coherent and squeezed light, adapted from the recent framework [14] proposed for Cesium.

2. Quantum enhanced fluorescence

2.1 Introduction

To properly assess the potential of squeezed light for realizing a Rubidium vapor-based two-photon clock, the realizable theoretical enhancement of quantum light over classical light is computed. In this regard, it is systematically assumed that conditions favor quantum operation (e.g. negligible linewidth broadening, atom cooled in a magneto-optical trap, four-level system) to put an upper bound on the quantum enhancement.

The energy level diagram of a Rubidium two-photon clock is given in Figure 1, which for the sake of simplicity is approximated as a four-level system whose transition parameters are summarized in Table 1. The clock transition is excited using two counterpropagating photons at 778 nm. The excited state then partially deexcites radiatively, emitting detectable fluorescence at 420 nm which is used as the control signal for locking the pump laser to the transition – a schematic representation of a potential implementation of a single-color two-photon clock is provided in Figure 2.

A quantum advantage of squeezed light is obtained if at equal pump photon flux, a higher fluorescence photon flux, results for a squeezed source compared to a classical source. Such an edge would enable Rubidium clocks to function at lower pump light power, potentially enabling lower SWaPs and, importantly, reducing the sensitivity of the clock to the Stark effect and leading to higher stabilities.

To determine the obtainable enhancement, the quantum optical scattering cross-section is first theoretically determined, permitting the excitation probability of the excited energy state to be computed for given pump conditions. From the excited state probability, a fluorescence photon flux can readily be determined. Simulations are conducted to solve the excitation probabilities and find the resulting quantum enhancements.

Table 1: Transition parameters relevant for the two-photon Rubidium clock

Transition	**Wavelength λ [nm]**	**Linewidth Γ [s^{-1}]**
$5S_{1/2} \rightarrow 5P_{3/2}$ (ab)	780.241	$38.11 \cdot 10^6$
$5P_{3/2} \rightarrow 5D_{5/2}$ (bc)	774.95	$2.89 \cdot 10^6$
$5D_{5/2} \rightarrow 6P_{3/2}$ (cd)	5233.10	$1.43 \cdot 10^6$
$6P_{3/2} \rightarrow 5S_{1/2}$ (da)	420.298	$1.873 \cdot 10^6$

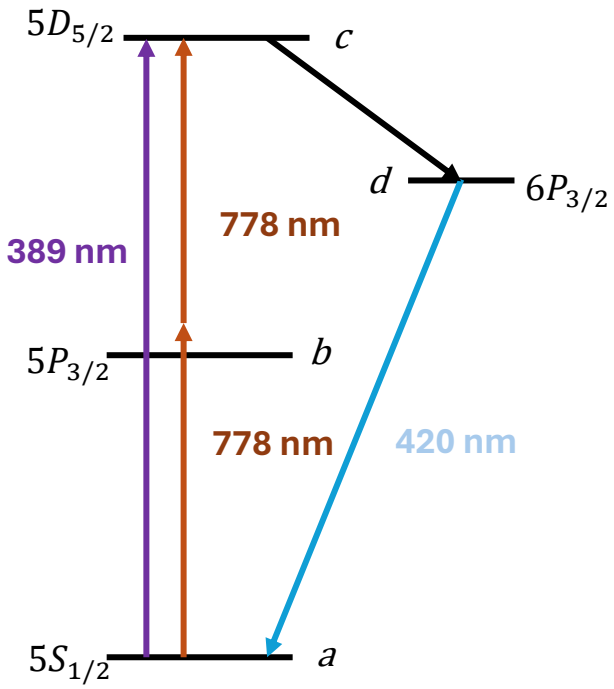

Figure 1: Energy level diagram of the two-photon Rubidium clock transitions.

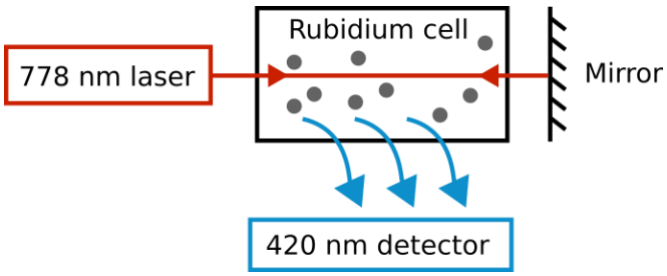

Figure 2: Possible implementation of an interrogation scheme for a Doppler-free, two-photon Rubidium clock. A 778 nm laser irradiates a Rubidium vapor cell and is reflected on a mirror, enabling photons from the incoming and reflected beam to probe the two-photon transition without contributions from the Doppler effect. The fluorescence resulting from the deexcitation of the two-photon excited Rubidium atoms can be detected with an appropriate detector and used to generate a control signal for tight stabilization of the pump laser to the atomic transition.

2.2 Excitation probability

It can be shown that [1] the excitation probability of the upper energy level is given by (up to a prefactor irrelevant to the current discussion)

$$p = \int L(\omega) \left| \int d\omega_I G_{ba}(\omega_I)\, a_{II}(\omega - \omega_I) a_I(\omega_I) |\Psi_{in}\rangle \right|^2 d\omega,$$

where

$$L(\omega) = \frac{1}{2\pi} \frac{\Gamma_c}{(\omega_{ca} - \omega)^2 + \frac{\Gamma_c^2}{4}}$$

corresponds to the two-photon transition lineshape, with

$$\Gamma_m = \sum_{n=a,b,c,d} \Gamma_{mn}$$

the total decay rate of state *m* (which can be *a, b, c* or *d*) with Γ_{mn} given in Table 1 and where the single-photon transition's lineshape from state *m* to state *n* is given by

$$G_{mn}(\omega) = \frac{1}{\omega_{mn} - \omega - i\frac{\Gamma_m}{2} - i\frac{\Gamma_n}{2}},$$

where $\omega_{mn} = 2\pi c/\lambda_{mn}$ and λ_{mn} given in Tab.1. To allow for a double color pumping scheme, a_i represent an annihilation operator centered around frequency ω_i. Finally, $|\Psi_{in}\rangle$ represents the initial state of the field. The excitation probability expression is understood as the integral over all possible two-photon annihilations summing to ω and weighted by the single photon intermediate state lineshape; and integrating over all possible ω weighted by the two-photon lineshape to sum up all contributions.

The fluorescence photon flux resulting from the excitation probability can be computed through the deexcitation pathways from the excited state as

$$f \propto p \frac{\Gamma_{da}^r}{\Gamma_d} \frac{\Gamma_{cd}}{\Gamma_c} N_{atoms}$$

with Γ_{da}^r the radiative contribution to the Γ_{da} linewidth and N_{atoms} the number of illuminated atoms. This equation can be straightforwardly understood, it carries the fact that **the fluorescence photon flux is given by the product of the excitation probability, the number of atoms, and the probability that the excited state deexcites through the fluorescent pathway**. Technically, exact fluorescence photon fluxes can be computed – but are unnecessary for the current analysis. As we are mostly interested in the enhancement that squeezed light can provide over classical light, it is sufficient to compute the excitation probability in both cases, as the deexcitation pathways of the excited level do not depend on how it has been excited.

2.3 Classical light

We now evaluate the excitation probability for the quantum state that is the closest to classical light, i.e. a coherent state. We start from a two-color classical light source modeled by coherent states

$$|\psi_{cl}\rangle = D_I(\alpha_I)D_{II}(\alpha_{II})|vac\rangle$$

with the displacement operator

$$D_J(\alpha_J) = e^{\alpha_J \int d\omega \phi_J(\omega) a^\dagger(\omega) - h.c.},$$

where $\phi_J(\omega)$ is the spectral distribution (i.e. the relative amplitude and phase) of the light sources, normalized so that

$$\int d\omega \left|\phi_J(\omega)\right|^2 = 1.$$

The average number of photons in each frequency band is then given by

$$N_J^{cl} = \int d\omega \langle\psi_{cl}|a_J^\dagger(\omega)a_J(\omega)|\psi_{cl}\rangle = \left|\alpha_J\right|^2,$$

while the two-point correlation function can be derived to be

$$\langle\psi_{cl}|a_I^\dagger(\omega_I')a_{II}^\dagger(\omega_{II}')a_{II}(\omega_{II})a_I(\omega_I)|\psi_{cl}\rangle = |\alpha_{II}|^2|\alpha_I|^2\phi_I^*(\omega_I')\phi_{II}^*(\omega_{II}')\phi_{II}(\omega_{II})\phi_I(\omega_I).$$

When replaced in the expression for the excitation probability, one gets

$$p_{cl} = |\alpha_I|^2|\alpha_{II}|^2 \int L(\omega)|\int G_{ba}(\omega_I)\phi_I(\omega_I)\phi_{II}(\omega-\omega_I)d\omega_I|^2 d\omega.$$

In the continuous wave limit, ϕ_J peaks at ω_J and the expression can be reduced to the excitation probability

$$p_{cw} = |\alpha_I|^2|\alpha_{II}|^2 L(\omega_I+\omega_{II})|G_{ba}(\omega_I)|^2.$$

This excitation probability under a finite photon flux is obviously maximized when $\omega_I = \omega_{ab}$ and $\omega_I + \omega_{II} = \omega_{ac}$ with $|\alpha_I|^2 = |\alpha_{II}|^2$ which corresponds to having half the photons pumping the single-photon transition and the other half pumping the single-photon excited state to the two-photon excited state. As stated earlier, this excitation probability is a direct measure of the resulting fluorescence signal.

2.4 Squeezed light

We suppose that the squeezed light is produced via *spontaneous parametric down-conversion* from a light source with frequency ω_p. In the continuous wave limit, each generated photon pair will be strongly correlated so that their frequencies $\omega_I + \omega_{II} = \omega_p$, which allows one to write the squeezed state as

$$|\psi_{sq}\rangle = e^{\beta e^{i\theta} \int d\omega_I \phi_I(\omega_I) a_I^\dagger(\omega_I) a_{II}^\dagger(\omega_p - \omega_I)},$$

with β the squeezing parameter, θ the squeezing angle and, under a Gaussian phase-matching with bandwidth Ω_c with center frequency $\bar{\omega}_J$ assumption,

$$\phi_J(\omega) = \sqrt{\frac{1}{\Omega_c}} e^{-\pi \frac{(\omega - \overline{\omega_J})^2}{2\Omega_c^2}}.$$

Defining

$$s_J(\omega) = sinh\left(\left|\beta \phi_J(\omega)\right|\right)$$

and

$$c_J(\omega) = cosh\left(\left|\beta \phi_J(\omega)\right|\right),$$

the average photon number is given by

$$N_J^{sq} = \int \frac{d\omega}{2\pi} s_J(\omega)^2.$$

Using the above definitions, it can be shown that the **excitation probability** consists of two terms. The first one is given by

$$p_{sq}^c = L\left(\overline{\omega_p}\right) \left| \int G_{ba}(\omega_I) e^{i\theta(\omega_I)} s_I(\omega_I) c_I(\omega_I) d\omega_I \right|^2$$

and is called the **coherent contribution**, as it represents the absorption of correlated photon pairs with energy summing to exactly the pump energy. Note that the integral is maximized when the squeezing angle is independent of frequency, and thus this assumption is made.

The second contribution to the excitation probability reads

$$p_{sq}^{ic} = \int L(\omega) \int |G_{ba}(\omega_I) s_{II}(\omega - \omega_{II}) s_I(\omega_I)|^2 \, d\omega d\omega_I$$

and represents the contribution of the **absorptions of uncorrelated photons**. Notably, the incoherent contribution is always smaller than the coherent one. As such, we put an upper bound on the excitation probability at twice the coherent excitation probability and forego the computation of the incoherent term.

2.5 Simulation settings

The above expressions for the excitation probability using classical and squeezed light can be used to simulate the expected highest quantum enhancement obtainable by using squeezed light to operate a two-photon clock. The only free parameters in the simulations are the number of photons and the bandwidth of the squeezed light.

The photon number, or more precisely, the photon flux will be numerically scanned to identify the regimes in which a quantum enhancement can be obtained. This leaves the bandwidth of squeezed light as a free parameter which will be studied in two cases, a low and a high bandwidth that will be defined later.

We investigate two options for the clock operation. In the first scenario, both light sources are non-degenerate, with photons equally distributed at the single photon transition and at the complementary energy to reach the peak of the two-photon transition. This configuration corresponds to a two-color two-photon clock and harnesses the enhancement in excitation offered by the single-photon resonance. However, this scheme has its own drawbacks, namely a more complex laser system and a possible implementation is illustrated in Figure 3

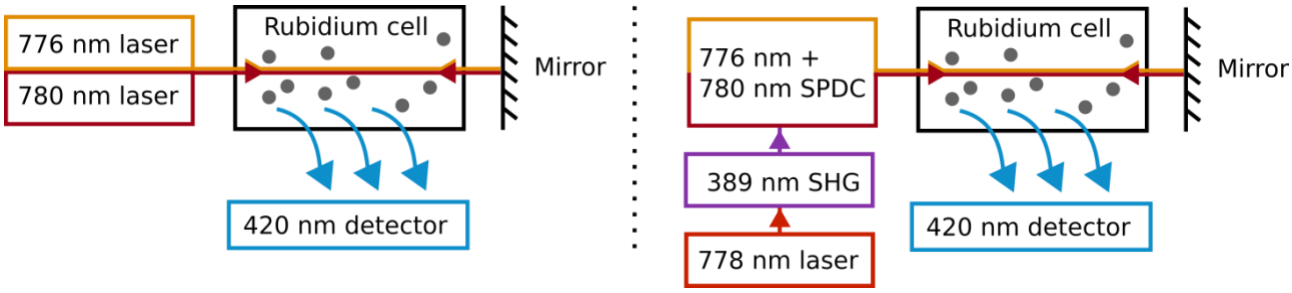

Figure 3: Possible implementation of a classical-light (left) and squeezed-light (right) two-color two-photon Rubidium clock corresponding to the first simulation scenario.

The second clock operation scheme assumes that both the squeezed and the classical light are degenerate, i.e. their spectra have a center frequency at half of the two-photon resonance frequency. This scheme is typically used in Doppler-free, single-color two-photon clocks. While this approach leverages lower enhancement from the single-photon transition, it requires only a single laser source and rids unwanted broadening effects, leading to simple laser systems, as seen in Figure 4.

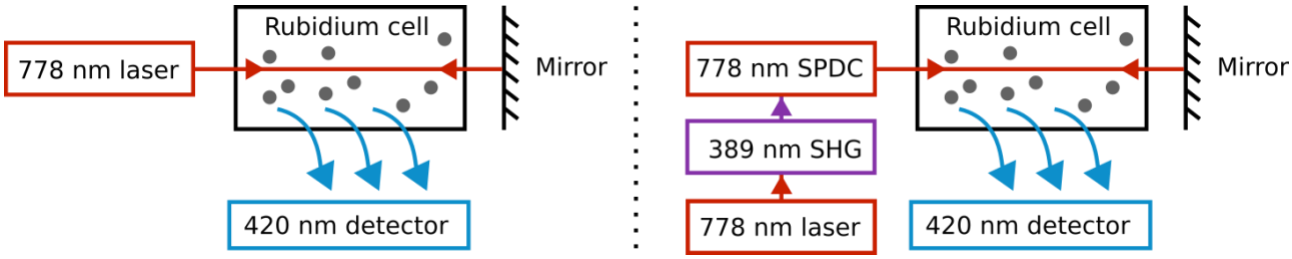

Figure 4: Possible implementation of a classical-light (left) and squeezed-light (right) two-color two-photon Rubidium clock corresponding to the second simulation scenario.

2.6 Low squeezed-light bandwidth

In this first simulation, we set the bandwidth of the squeezed source to be equal to the linewidth of the single-photon transition. The results are displayed in Figure 5.

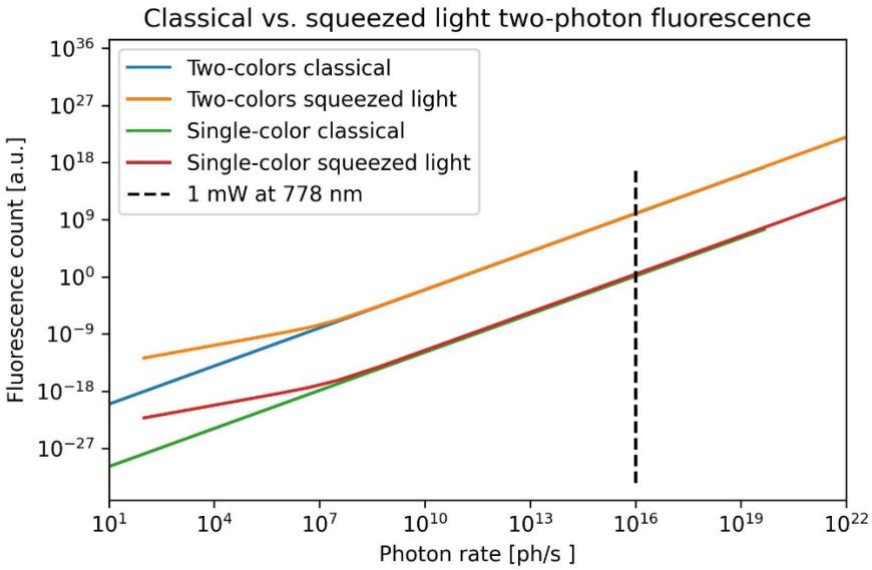

Figure 5: Simulations results. The fluorescence rates obtained in different pumping configurations are displayed, with a squeezed light bandwidth equal to the linewidth of the single-photon transition.

An immediate result, which is also evident from its theoretical expression, is that fluorescence generated from classical light always scales quadratically with the photon number. This can also be understood from the observation that two-photon absorption is a cubic nonlinear process, thus scales with the square of the light's intensity. Intuitively, as a photon cannot excite the transition alone, the fluorescence rate depends on the probability that two photons arrive at the same time which scales as the square of the light's intensity.

Comparing the results obtained from degenerate and non-degenerate classical pump sources, we can easily observe that **the enhancement provided by the single-photon transition (acting as a resonant 'ladder' for the excitation) results in fluorescence rates enhanced by orders of magnitude**.

At very low photon numbers, one can directly see that squeezed light provides a significant enhancement to the fluorescence rate. As the spontaneous parametric down-conversion process generates pairs of entangled photons, a photon is always accompanied by another photon with the complementary energy to reach the two-photon transition. As such, the probability of having two photons arriving at the same time is the same as the probability of having a single photon, which scales linearly with the intensity. This is observable in the rate of the fluorescence rate growing linearly with the photon number at low photon numbers.
At higher photon fluxes, different photon pairs start arriving simultaneously in the Rb atoms. When this is the case, the photons absorbed can either be from an entangled pair, or two photons from different entangled pairs. Of course, this last situation is fully analogous to the classical case and scales with the square of the light intensity, resulting in a behavior very similar to classical light at high photon numbers.

At this low squeezed-light bandwidth, it can also be shown that the asymptotic enhancement provided by squeezed light at high photon numbers is a factor of 2.

We note that for a typical operation point of a degenerate two-photon Rubidium clock, one uses a classical light source with around 1 mW or more of power to excite the transition and get acceptable signal-to-noise ratio on the resulting fluorescence. As such, this operation point has been reported in terms of photon flux as a vertical dashed line in 5. One observes that at this operation point, we can estimate the quantum enhancement to be around a factor of 2.

As all estimations and approximations carried out so far are highly in favor of the quantum enhancement, it is quite clear that a factor of 2 is highly optimistic and not experimentally feasible, and as such, **squeezed light with low bandwidth is not expected to bring an edge to a two-photon Rubidium clock operating at reasonable parameters with a classical light source**.

2.7 High squeezed-light bandwidth

To complete the study, we turn towards an extreme case where the bandwidth of the squeezed light spans across multiple nanometers, such that degenerate squeezed light covers the single-photon transition. In this case, we obtain the results displayed in Figure 6.

Of course, classical light-produced fluorescence behavior is identical to the results discussed earlier. However, squeezed light displays a different behavior – in this case, the bandwidth of the squeezed light enables both the non-degenerate and the degenerate cases to populate the frequencies of the single-photon transition, which results in the two cases being almost identical. One can notice slightly better results for the degenerate squeezed light, as all its photons have a bandwidth that contains both the single-photon transition and the complementary transition from the single-photon excited state to the two-photon excited state.

Interestingly, this large bandwidth enhances the degenerate squeezed-state fluorescence rate through better overlap with the single-photon transition. On the contrary, the non-degenerate squeezed-state fluorescence is degraded, as an extension of its bandwidth results in a worst distribution of energy inside the single-photon transition bandwidth.

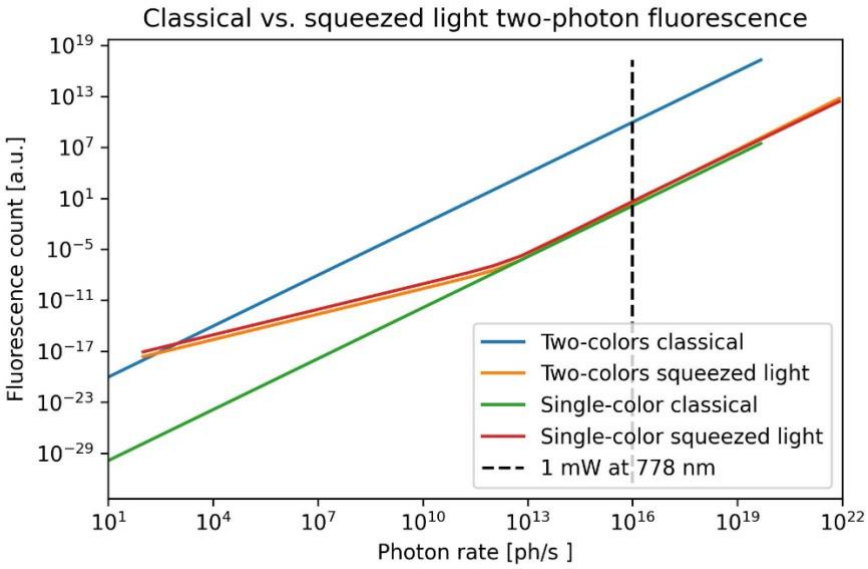

Figure 6: Simulation results. The fluorescence rates obtained in different pumping configurations are displayed, with a squeezed light bandwidth spanning multiple nanometers.

It can also be seen that the squeezed states are heavily outperformed by the two-color classical light at all photon numbers, and extremely close to the degenerate classical case, once again providing little incentive to pursue squeezed-light illumination in a two-photon Rubidium clock.

3. Quantum intermodulation noise reduction

3.1 Introduction

Intermodulation noise is a fundamental limit to the performances of clocks relying on a modulation scheme to probe an atomic transition. The phase noise of the oscillator (for optical clocks, the laser source) at twice the modulation frequency contaminates the error signal and affects the quality of the lock of the oscillator to the atoms. This effect can result in a degradation of the short-term stability of two-photons Rubidium clock.

We investigate here how quantum light can potentially help to reduce intermodulation noise through phase noise squeezing.

3.2 Intermodulation effect

As a reminder, we follow here loosely the derivation of [15] to find the intermodulation noise in terms of phase noise of the laser source used.

We define $\omega(t)$ as the instantaneous frequency of the laser source and ω_0 as the resonance frequency of the atomic transition, which also corresponds to the mean of $\omega(t)$ if control loops work properly. Then, the instantaneous frequency deviation $\omega(t) - \omega_0$ contains different contributions, one of them being the deliberately imprinted modulation, which we denote by $\omega_m g(t)$, where ω_m is the modulation depth and $g(t)$ the periodic modulation function of frequency f_M and with maximum absolute value of unity and an odd function of time. We can then separate the remaining

frequency fluctuations as $\omega_s(t)$ and $\omega_f(t)$, representing slow, respectively fast frequency fluctuations (where slow is defined to correspond to the locking bandwidth). The frequency deviations are then given by

$$\omega(t) - \omega_0 = \omega_m g(t) + \omega_s(t) + \omega_f(t).$$

Practically, ω_m is set to around half the atomic transition linewidth W, which for typical laser sources implies

$$\omega_s(t), \omega_f(t) \ll \omega_m.$$

The time-dependent response of the atomic resonator is then

$$\frac{I(t)}{I_0} = h\left(\frac{\omega(t) - \omega_0}{W}\right),$$

with h an even function of the frequency detuning. At first order, this can be expanded into

$$\frac{I(t)}{I_0} = h\left(\frac{\omega_m}{W} g(t)\right) + \left(\omega_s(t) + \omega_f(t)\right) \frac{\partial h(\omega_m g(t)/W)}{\partial \omega}.$$

From the given assumptions, the first term does not contain components at frequency f_M, while the second term does. By selectively filtering the response around f_M, we thus get

$$\frac{I'(t)}{I_0} = \left(\omega_s(t) + \omega_f(t)\right) \sum_n P_{2n+1} sin(2\pi(2n+1) f_M t),$$

where P_{2n+1} are Fourier coefficients that can be computed from h, $g(t)$ and ω_m. The fast fluctuation can be decomposed in the Fourier base, and we define their in- and out-of-phase Fourier amplitude at $2f_M$ by q_{2fM} and p_{2fM} respectively. One can then show that the fluctuations of the response of the atomic resonator at frequency f_M is given by (keeping only the leading terms)

$$\frac{I_{fM}(t)}{I_0} = P_1 \omega_s(t) sin(2\pi f_M t) - \alpha q_{2fM}(t) sin(2\pi f_M t) - \beta p_{2fM}(t) cos(2\pi f_M t),$$

where α and β can be computed from the P_n coefficients. After demodulation at $sin(2\pi f_M t)$, we obtain an error signal that is forced to zero by the control loop, which gives

$$\omega_s(t) = \frac{\alpha}{P_1} q_{2fM}.$$

This demonstrates that even with a closed control loop forcing the demodulated signal at zero, we obtain residual frequency fluctuations that directly depend on the noise amplitude of the laser source at $2f_M$. From the assumption that this noise is white, one can show that the resulting residual Allan deviation from this frequency instability is given by

$$\sigma_y(\tau) \approx \sqrt{S_y(2f_M)}/2\sqrt{\tau},$$

demonstrating that the frequency (or phase) noise of the source at $2f_M$ perturbs the frequency stability of the clock.

Importantly, this formula also allows one to compute potential enhancements to the stability coming from improvements in the source's phase noise.

3.3 Quantum light phase noise reduction

By using a quantum source, it is possible to obtain phase noise below what is achievable by a classical light source, which from the results above should directly improve the intermodulation limit to the clock stability.

The standard approach to squeezed light assumes squeezing in one of the quadratures of the electric field. Unfortunately, such a definition of a squeezed state does not allow for a simple computation of the associated phase noise reduction. In fact, while some forms have been proposed (see e.g. [16]), it is not clear that a proper quantum phase operator can be defined – and resulting computations promise tediousness.

As such, we follow here an alternative approach that should provide reasonable insight into the enhancement in phase noise that can be obtained, based on an analysis of the phase space of squeezed light.

We start with the standard expression of the quantum harmonic oscillator Hamiltonian, which will be the starting point of our discussion:

$$\mathrm{H} = \hbar\omega\left(a^\dagger a + 1/2\right).$$

Note that $n = a^\dagger a$ is the photon number operator and will be used later. One can then define the quadrature operators $X = \left(a^\dagger + a\right)/2$ and $Y = \left(a - a^\dagger\right)/2i$ to write

$$H = \hbar\omega(X^2 + Y^2),$$

these quadrature operators obey the Heisenberg uncertainty principle

$$\Delta^2 X \Delta^2 Y \geq 1/16.$$

A coherent state (classical light) saturates the inequality and has $\Delta^2 X = \Delta^2 Y = 1/4$. This allows one to draw the phase-space diagram of a coherent state as in Figure 7.

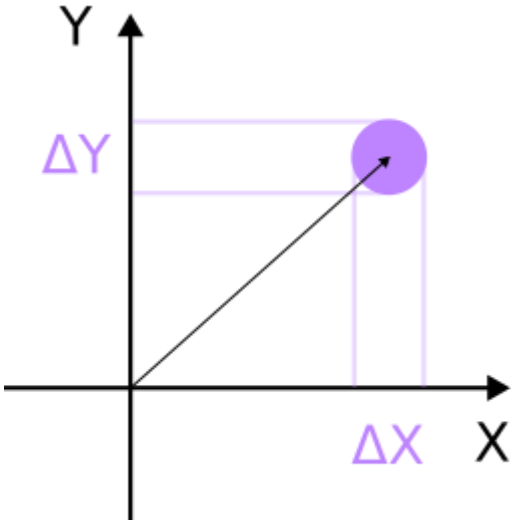

Figure 7: Phase-space of a coherent state.

Squeezed light, by definition, is a state that has a quadrature component (or a combination of them) with variance smaller than ¼. Supposing for instance a squeezing in the X operator, the phase-space diagram can be drawn as in Figure 8.

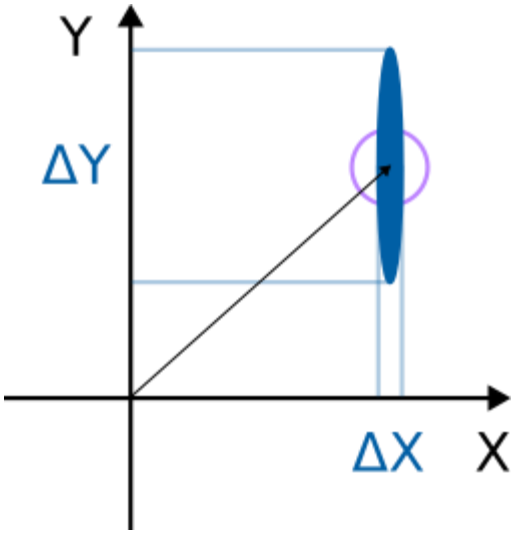

Figure 8: Phase-space representation of an X-squeezed state.

To get an insight into potential phase noise reduction induced by squeezing, we first note that from the Heisenberg time-energy uncertainty relation

$$\Delta E\, \Delta t \geq \hbar/2$$

evaluated with an n-photon state, we have $\Delta E = \hbar\omega\Delta n$, while the phase $\phi = \omega t$ implies $\Delta t = \Delta\phi/\omega$ and thus

$$\Delta n\, \Delta\phi \geq 1/2.$$

Consequently, we see that a state that is squeezed in phase, thus with reduced phase noise, must be anti-squeezed in the photon number, and thus have higher intensity noise. Notably, this type of

light is often called super-Poissonian light, as it exhibits a photon number distribution with a variance higher than that of a standard Poisson distribution.

Noting that $n = X^2 + Y^2 - 1/2$, the photon number in the phase space is readily identified as the analogous of the squared radius from the origin to the center of the phase space region occupied by the state of interest. Similarly, the phase can be identified as the polar angle at which the phase space is occupied, as depicted in Figure 9.

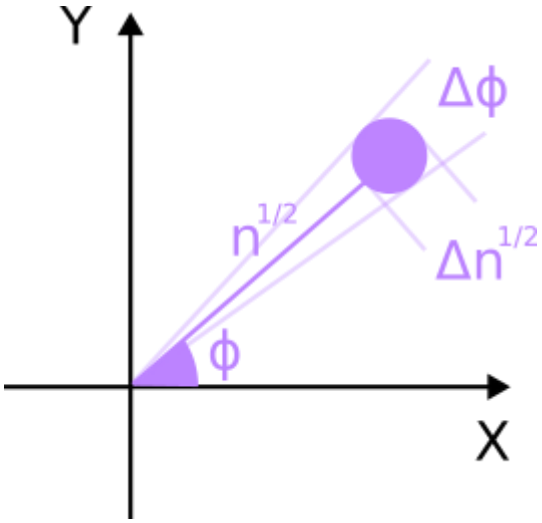

Figure 9: Photon number and phase representation of a coherent state in the quadrature phase-space.

It is then directly seen that the phase noise is minimized when the orientation of the anti-squeezing points towards the origin, as in Figure 10.

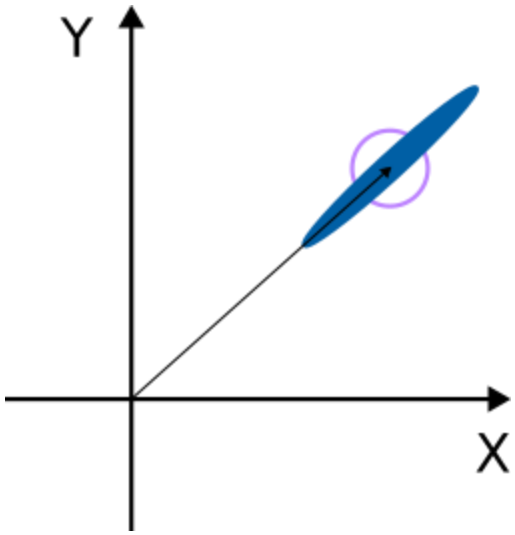

Figure 10: Maximally phase-squeezed state phase-space representation.

Practically, if the squeezing angle can be modified without changing the overall phase, then it is possible to orient the squeezing direction to minimize the resulting phase noise. We note that squeezing experiments conducted so far have achieved quadrature squeezing enhancements of a few dB, which we will optimistically estimate to translate to 5 dB in an experiment on a two-photon clock. We can then estimate the potential photon number noise reduction to be on twice the same

order, i.e. 10 dB. If the squeezing can be rotated freely in the phase space, then we can estimate the potential phase noise reduction to be on the same order of 10 dB, from the above Heisenberg uncertainty principle.

Combined with the results obtained in the intermodulation section, using squeezed-phase light should provide an enhancement of the two-photon clock intermodulation-limited stability scaling with the square root of the squeezing factor. Optimistically, **this could result in up to 5 dB of quantum enhancement of the two-photon clock stability**, provided its stability is limited by the intermodulation noise.

4. Conclusion

We have demonstrated via theoretical derivation and subsequent simulations that quantum light should not provide meaningful enhancements to the fluorescence rates of two-photon Rubidium optical clocks. In typical operating conditions, the analysis shows that two-color classical excitation light is the preferred approach. However, this approach has several technical drawbacks, including using two distinct lasers. This encourages us to pursue the single-color approach which has a higher potential for a low SWaP, without compromising significantly on the short-term stability.

In addition, we have studied the intermodulation noise, originating from the phase noise of the laser source used to probe the atomic transition. A direct approximation of its contribution to the stability of the clock is given. The phase-space representation of quantum squeezed sources is then used to derive an upper bound on the potential of quantum sources to reduce the intermodulation noise. Provided the clock stability is limited by the intermodulation noise, we could expect at most an enhancement of a few dB, directly linked to the square root of the practically achievable squeezing parameter.

References

(1)
Entangled Two-Photon Absorption Spectroscopy | Accounts of Chemical Research. https://pubs.acs.org/doi/abs/10.1021/acs.accounts.8b00173 (accessed 2025-12-23).
(2)
Entangled photon spectroscopy - IOPscience. https://iopscience.iop.org/article/10.1088/1361-6455/aa8a7a (accessed 2025-12-23).
(3)
Dorfman, K. E.; Schlawin, F.; Mukamel, S. Nonlinear Optical Signals and Spectroscopy with Quantum Light. *Rev. Mod. Phys.* **2016**, *88* (4), 045008. https://doi.org/10.1103/RevModPhys.88.045008.
(4)
Dayan, B. Theory of Two-Photon Interactions with Broadband down-Converted Light and Entangled Photons. *Phys. Rev. A* **2007**, *76* (4), 043813. https://doi.org/10.1103/PhysRevA.76.043813.
(5)
Fei, H.-B.; Jost, B. M.; Popescu, S.; Saleh, B. E. A.; Teich, M. C. Entanglement-Induced Two-Photon Transparency. *Phys. Rev. Lett.* **1997**, *78* (9), 1679–1682. https://doi.org/10.1103/PhysRevLett.78.1679.
(6)
Schlawin, F.; Mukamel, S. Photon Statistics of Intense Entangled Photon Pulses. *J. Phys. B: At. Mol. Opt. Phys.* **2013**, *46* (17), 175502. https://doi.org/10.1088/0953-4075/46/17/175502.
(7)
Oka, H. Two-Photon Absorption by Spectrally Shaped Entangled Photons. *Phys. Rev. A* **2018**, *97* (3), 033814. https://doi.org/10.1103/PhysRevA.97.033814.
(8)
Lee, D.-I.; Goodson, T. Entangled Photon Absorption in an Organic Porphyrin Dendrimer. *J. Phys. Chem. B* **2006**, *110* (51), 25582–25585. https://doi.org/10.1021/jp066767g.
(9)
Parzuchowski, K. M.; Mikhaylov, A.; Mazurek, M. D.; Wilson, R. N.; Lum, D. J.; Gerrits, T.; Camp, C. H.; Stevens, M. J.; Jimenez, R. Setting Bounds on Entangled Two-Photon Absorption Cross Sections in Common Fluorophores. *Phys. Rev. Appl.* **2021**, *15* (4), 044012. https://doi.org/10.1103/PhysRevApplied.15.044012.
(10)
Mikhaylov, A.; Wilson, R. N.; Parzuchowski, K. M.; Mazurek, M. D.; Camp, C. H.; Stevens, M. J.; Jimenez, R. Hot-Band Absorption Can Mimic Entangled Two-Photon Absorption. arXiv January 30, 2022. https://doi.org/10.48550/arXiv.2111.05946.
(11)
Hickam, B. P.; He, M.; Harper, N.; Szoke, S.; Cushing, S. Single Photon Scattering Can Account for the Discrepancies Between Entangled Two-Photon Measurement Techniques. *J. Phys. Chem. Lett.* **2022**, *13* (22), 4934–4940. https://doi.org/10.1021/acs.jpclett.2c00865.
(12)
Landes, T.; Smith, B. J.; Raymer, M. G. Limitations in Fluorescence-Detected Entangled Two-Photon-Absorption Experiments: Exploring the Low- to High-Gain Squeezing Regimes. *Phys. Rev. A* **2024**, *110* (3), 033708. https://doi.org/10.1103/PhysRevA.110.033708.
(13)
How large is the quantum enhancement of two-photon absorption by time-frequency entanglement of photon pairs? https://opg.optica.org/optica/fulltext.cfm?uri=optica-8-5-757 (accessed 2025-12-23).

(14)
Drago, C.; Sipe, J. E. Fluorescence Driven by Nonclassical Light. arXiv August 16, 2025. https://doi.org/10.48550/arXiv.2508.12037.
(15)
Audoin, C.; Candelier, V.; Diamarcq, N. A Limit to the Frequency Stability of Passive Frequency Standards Due to an Intermodulation Effect. *IEEE Transactions on Instrumentation and Measurement* **1991**, *40* (2), 121–125. https://doi.org/10.1109/TIM.1990.1032896.
(16)
Ma, X.; Rhodes, W. Quantum Phase Operator and Phase States. arXiv April 23, 2016. https://doi.org/10.48550/arXiv.1511.02847.

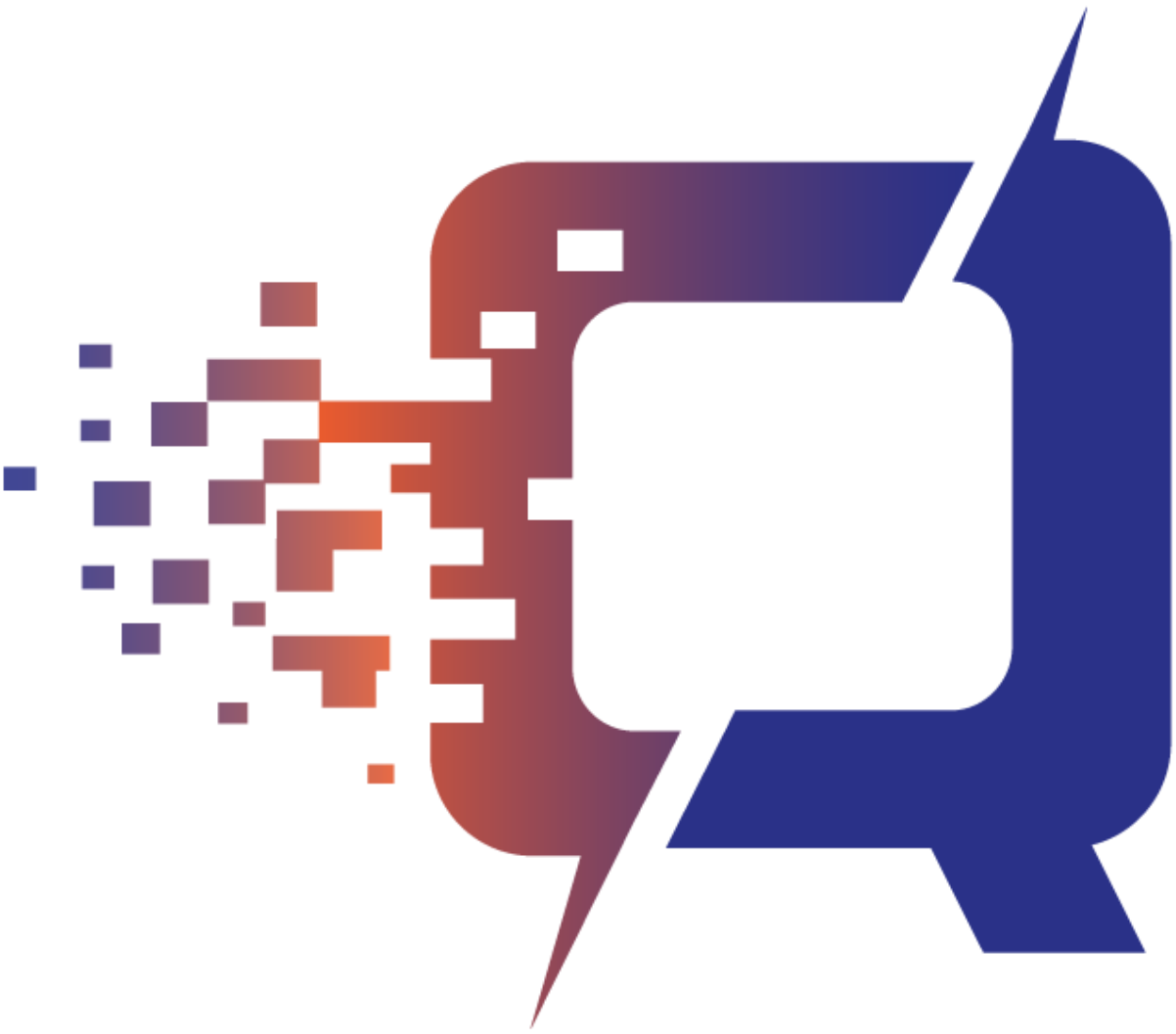

QUantum Enh**AN**ced
Pho**T**onic **I**ntegrated Sensors
For Metrolog**Y**